Project title: Smart Optical and Ultrasound Diagnostics of Breast Cancer

Grant Agreement: 731877

Call identifier: H2020-ICT-2016-1

Topic: ICT-29-2016 Photonics KET 2016

Deliverable 4.1: Design of multi-modal phantoms for DOT-US

Leader partner:	Beneficiary 1, POLIMI
Author(s):	Alberto Dalla Mora (POLIMI), David Savery (SSI)
Work Package:	4
Estimated delivery:	Month 6
Actual delivery:	28 April 2017
Type:	Report
Dissemination level:	Public

Tables of contents

Abbreviations

DOT   Diffuse Optical Tomography

SOS   Speed Of Sound

US   Ultrasound

1. Introduction

This first WP4 deliverable aims to find out materials and solutions that can allow the fabrication of phantoms suitable for working with two techniques at the basis of the SOLUS project: diffuse optical tomography (DOT) and ultrasound (US). These preliminary investigations will then allow the development of a kit of phantoms (D4.4, due at M18) suitable to anticipate and solve problems and to optimize the SOLUS system before the clinical validation. The kit will be used in particular for an objective assessment of instrument performances against specific clinically-related targets (defined in D2.1, delivered at M4) thanks to the definition of protocols for the performance assessment of DOT and of combined DOT-US systems (D4.2, due at M12) and of simplified protocols for daily routine tests in clinical settings (D4.3, due at M18).

Different solutions for DOT phantoms and US phantoms are already available in the literature and also at commercial level, but a phantom validated with both modalities is still lacking. The effort in finding the best solution for joint phantoms is motivated by the main goal of WP4, which is the validation in laboratory settings of SOLUS technologies and of the final prototype. To this purpose, similarly to a real measurement performed on breast, it is important to combine the two techniques on the same phantom to allow exploiting the US acquisition of morphology as an *a priori* information for DOT.

This report is organized as follows: Section 2 deals with requirements of phantoms in terms of the clinical paradigm to be implemented and needs of the two techniques; Section 3 reports the US characterization of different materials that can be suitable to DOT; Sections 4 deals with fabrication process and layout of a first prototype of phantom potentially working with the two modalities; Section 5 reports the optical and US characterization of the first phantom fabricated; Section 6 shows the design and US characterization of a second-level prototype designed to overcome problems of the first prototype; finally, conclusions are discussed in Section 7.

2. Phantom Requirements and Options

In order to evaluate materials and solutions for the design of phantoms, it is important to define the general requirements and the needs of both DOT and US.

As a general requirement, it is desirable to use materials that can allow us to obtain durable phantoms, thus avoiding the fabrication of new phantoms every time they are needed and the related repeatability issues. To this purpose, it is desirable to try to avoid liquid phantoms or water-based gels like agar-based phantoms due to alterations coming from both bacteria and water evaporation. In addition, to mimic the presence of a lesion in the breast, we need the possibility to embed heterogeneities into the medium. These have to be visible to both US and DOT. When using liquid phantoms, this is possible only using membranes to separate different phantom compartments, thus possibly introducing artefacts in the DOT measurements due to the presence of such a membrane. Thin (<150 µm) Mylar sheets have been extensively validated in diffuse optics to separate different layers of liquid phantoms. However, with such material it is not trivial to fabricate holders for localized perturbations.

As defined in D2.1 "Definition of paradigms representing exemplary breast lesions cases", representative lesion morphologies have been identified. In particular, a round shape of the inclusion will be considered as a first approximation, with a minimum diameter of 1 cm. For the minimum dimension, the centre of the inclusion could be located at a typical depth of 1.0 ± 0.5 cm, while, for bigger sizes, the top of the inclusion could be located at a typical depth of 1.5 ± 0.5 cm. For fabrication of heterogeneous phantoms, it is possible to consider cylindrical inclusions for simplicity.

Additionally, each technique has its own particular requirements to be considered.

DOT requires well-controllable optical properties in the phantom fabrication. For both the bulk phantom and for the inclusion, ideally the main material should be transparent and non-diffusive in the whole wavelength range addressed by the application. The possibility is also required to embed scattering centres using powders (like TiO2 particles) or fat emulsions (like Intralipid) and absorption centres (like black toner powder or inks). These components must be added at the proper concentration and

homogeneously distributed in the phantom, thus ensuring to obtain the desired values of both absorption coefficient (μ_a) and reduced scattering coefficient (μ_s').

US phantoms are typically used to assess the system performance in terms of spatial resolution and sensitivity. To this purpose, they should fully mimic tissue properties in terms of attenuation, echogenicity, acoustical impedance mismatch of inclusions, speed of sound. Although in the longer run it may be desirable to replace these standard phantoms working only with US with new phantoms working with both techniques, the main goal now is to fabricate phantoms allowing the US measurement for extracting the morphological information, without the need to match all the characteristics of phantoms routinely used for US performance assessment. To this purpose: i) attenuation should be sufficiently low to allow US penetration down to a depth of few centimetres; ii) echogenicity and/or acoustical impedance mismatch of inclusion should be sufficient to highlight the shape and size of the simulated lesion to extract the morphological information; iii) since the speed of sound of the investigated material can usually be set on the US machine, its value should be in the tuning range of the developed SOLUS system.

3. US Properties Characterization of Materials

INTRODUCTION

Considering the requirements of using solid phantoms to minimize degradation over time, we started reviewing materials already validated for diffuse optics applications. Among these, epoxy resins and silicone rubbers have been widely used [1]-[5]. Unfortunately, looking at values tabulated in the literature for this kind of materials, an excessive SOS is expected for epoxy resins and, in particular, a strong attenuation of the US signal. For silicone rubbers, a quite low SOS is expected, but possibly in the tuning range allowed by the SOLUS system [6].

Hydrogel phantoms have also been proposed for simulating both optical and ultrasonic properties of human tissues. Their preparation can be complex and they have to be kept in a fridge to preserve them from degradation [7]. So they can be effective for laboratory use, but the purpose here is the fabrication of a phantom kit with many samples, which enables measurements repeated over time, can be shared between laboratories, and exploited in a clinical environment. So, if possible, the phantom properties should not be affected when they are stored at room temperature.

Finally, urethane rubber proved suitable to replicate US properties of tissues [8], but it is usually not water-clear as it might be desirable with the purpose to fabricate phantoms with well controlled optical properties in the whole spectrum of interest for SOLUS. However, we were able to find a commercially available water-clear urethane rubber (Smooth-On, www.smooth-on.com) that has been added to other materials under test since it could feature suitable US properties.

Here, different material samples were tested as candidates for raw material to fabricate phantoms compatible for ultrasonic and optical imaging. First of all, we evaluated acoustical properties of some materials and then chose the best candidate for optical imaging. Several cylindrical samples of the different materials with average diameter of 60 mm and average height 14 mm were tested.

MATERIALS

A laboratory SSI Aixplorer V11 (S/N: SIA4115) was used, together with a SSI SL15-4 Gen. 1 linear ultrasound probe (S/N: 954F1105, 256 elements probe, element pitch 0.2 mm, resonance frequency 8.0 MHz, relative -6 dB bandwidth 80%).

A laboratory set-up normally used for US probe characterization was used. This set-up includes: i) a flat stainless steel reflector, ii) a 3 rotation angles manual mechanism to control the probe orientation, iii) a linear stage controller to set the distance of the flat reflection with respect to the probe surface.

A commercial phantom CIRS 040GSE was used as a reference for US scattering properties measurement.

The probe and the mechanical set-up including the flat reflector are immersed in degassed water (temperature range: 20 to 26°C). A distant personal computer communicating with the Aixplorer software and a special MATLAB software were used to properly align the axis of the probe and the normal axis of flat reflector using adequate ultrasound pulses and by manually controlling the probe orientation.

The sample to test is lying on the surface of the flat reflector between the probe and the reflector. A layer of water of about 30 mm thickness separates the probe from the sample surface.

Samples tested are:

1) pure water as a reference;

2) silicone Sylgard S528 firm gel, Dow Corning (Part A and B 50:50 ratio, optical properties μ_s' ~ 10 cm^{-1} adding TiO$_2$ powder; μ_a ~ 0.1 cm^{-1} adding carbon black silicone);

3) silicone Sylgard S184 elastomer, Dow Corning (Part A and B 10:1 ratio, optical properties μ_s' ~ 10 cm^{-1} adding TiO$_2$ powder; μ_a ~ 0.1 cm^{-1} adding carbon black silicone);

4) silicone Sylgard S184 elastomer, Dow Corning (Part A and B 10:0.5 ratio, modified recipe to reduce hardness trying to tune SOS, optical properties μ_s' ~ 10 cm^{-1} adding TiO$_2$ powder; μ_a ~ 0.1 cm^{-1} adding carbon black silicone);

5) epoxy resin NM ME 500/NM Hardare 179B, Nils Malgrem AB (Part A and B 10:3.5 ratio, optical properties μ_s' ~ 7.5 cm^{-1} adding TiO$_2$ powder; μ_a ~ 0.1 cm^{-1} adding black toner powder);

6) P-4 silicone rubber, Silicones Inc. (Part A and B 10:1 ratio, optical properties μ_s' ~ 7.5 cm^{-1} adding TiO$_2$ powder; μ_a ~ 0.1 cm^{-1} adding carbon black silicone);

7) Clear Flex 30 Urethane Rubber, Smooth-On (Part A and B 100:94 ratio, clear with no addition of scattering particles or absorbers), the index of refraction of the final rubber is about 1.486 at 25°C.

METHODS

The water SOS is assumed to be c_0 = 1480 m/s (+/- 1%). A substitution method is used to measure the material SOS. Acoustical pulses with B-mode breast imaging characteristics are fired toward the sample. For each pulse, several receive echoes can be measured:

  • the pulse that is created at the water-phantom interface is received at a time t_S that corresponds to the pulse traveling through the double distance between the probe and the phantom (t = 0 corresponds to the pulse transmission).

  • a transmitted pulse travels through the phantom material of thickness h, is reflected back by the flat reflector, travels the material thickness h and goes back to the probe. The echo of the flat reflector is received at a time t_1.

A measurement is performed without material sample to record the echo of the flat reflector though water only, its arrival time is labelled as t_0.

Three times of acoustical propagation are measured t_1, t_0, t_S. They can be transformed in equivalent depth measurements z_1, z_0 and z_S by computing: $z_1 = c_0 t_1/2$; $z_2 = c_0 t_2/2$; $z_S = c_0 t_S/2$. They are the equivalent depths measured on input images.

The material speed of sound c_1 can then be estimated by: $c_1 = c_0/[1 + (z_1 - z_0)/h]$, where h is the material thickness estimated by: $h = z_0 - z_S$.
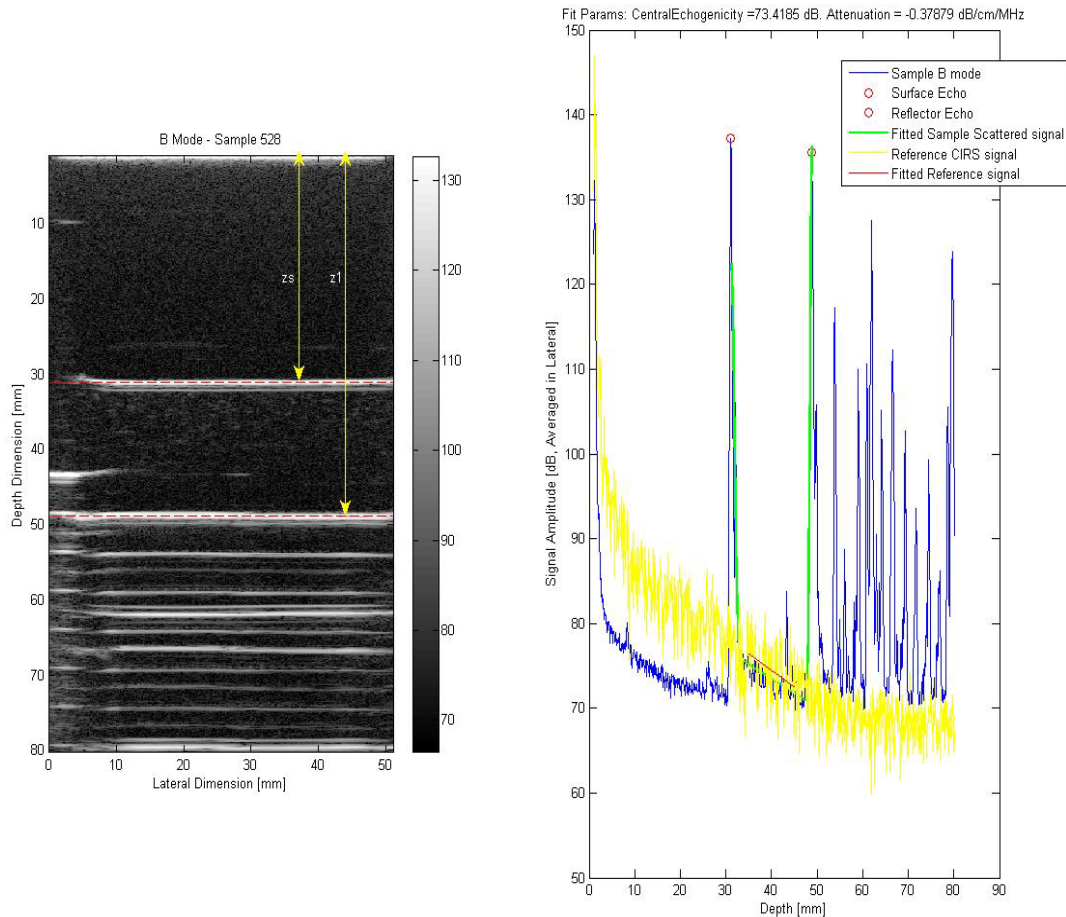
Figure 1 Example of B mode image of sample (left) and relative scatter measurements (right).

A relative method is used to measure the material scattering and attenuation property at the central frequency of 9.0 MHz. Two amplitude images are used: one with the set-up of the phantom experiment, and an ultrasound image of a section of the reference phantom CIRS GES040 in the 0.5 dB/cm/MHz attenuation portion, taken in the same condition as the other experiments.

The characteristics of the excitation voltage correspond to the optimized settings used on Aixplorer breast application preset. The central frequency of the excitation voltage is 9.0 MHz, the pulse amplitude is 72 V, the pulse duration is 0.11 μs. The focal length is set at 60 mm, the transmit aperture is 17.2 mm x 4.0 mm and the transmit apodization corresponds to a Hanning window. The assumed speed of sound for image reconstruction is 1480 m/s.

To characterize material echogenicity and ultrasound attenuation, the B mode amplitude in dB was modelled as a function of depth inside the phantom material by a linear function of depth. This variation was characterized by the amplitude in dB at the centre of the sample and by a negative slope in dB/cm. The amplitude at the centre of the sample was compared to the amplitude at the same depth in a reference phantom to obtain the relative echogenicity of the material at the transmit frequency. This slope was normalized by the transmit central frequency and divided by two to obtain the medium attenuation in dB/cm/MHz.

Only for the Clear Flex 30 Urethane Rubber, since the material attenuation was very strong (not quantitatively measurable), we had problems in identifying the return echo, confounded between echoes coming from the tank boundaries. Another approach was therefore taken with a smaller sample. The SOS was estimated by cutting a 4 mm thick slice of the sample and measuring it with the US probe. The SOS setting in the Aixplorer system was finely tuned until the thickness of the B-mode image reported the correct value of the slice thickness.

Table 1 US performances measured on the different materials under test.

Sample	SOS (m/s)	SOS uncertainty (m/s)	Attenuation (dB/cm/MHz)	Relative echogenicity (dB; 0dB = CIRS040GSE)
Water	1480	15		
S582	1013	30	0.60	2.2
S184 (10:1)	1028	31	0.45	-2.4
S184 (10:0.5)	1029	31	0.55	-2.4
Epoxy Resin	2696	81	10.70	11.4
P4	1119	34	0.15	-4.5
Clear Flex 30	1480		Not measurable	Not measurable

As an example of the measurements performed, Figure 1 (left) shows a B mode image taken from the top of a cylindrical phantom. The white line at depth z_s is an echo coming from the top of the phantom material. The upper part of the image (depth zero to z_s) corresponds a layer of water, the intermediate part of the image from z_s to z_1 corresponds to the phantom material. The while line at z_1 corresponds to the phantom/steel reflector. The Figure 1 (right) corresponds to laterally-averaged amplitude of the phantom material images and of the reference CIRS phantom (in dB).

RESULTS AND DISCUSSION

Table 1 reports measurement results on various materials tested and the SOS value of pure water for comparison. As expected, we found a very high SOS and attenuation for epoxy resin, together with a quite low SOS in all the measured silicone rubbers. Considering the acceptance range for the SOS (i.e. 1000-2000 m/s), it is worth noting that all silicone rubbers and the Clear Flex 30 urethane rubber can be used. However, the strong attenuation of the US signal prevented the acquisition of other features like the relative echogenicity. In principle, an acceptance range for the relative echogenicity could be from -3 up to 3 dB (i.e. not too far from the reference phantom echogenicity), thus excluding the P4 phantom. However, as already stated, the purpose now is not to replace standard US phantoms with these new phantoms, but the main goal for the project is to fabricate phantoms allowing the US measurement for extracting the morphological information, without the need to match all the characteristics of phantoms routinely used for US performance assessment.

CONCLUSION

Notwithstanding the low SOS, all the silicone rubbers tested were identified to be compatible with US imaging requirements. Clear Flex 30 urethane rubber, initially considered thanks to its water-clear transparency that probably makes it suitable for DOT, showed the same SOS of pure water, but the strong attenuation to US propagation can possibly prevent its use in joint DOT-US phantoms.

4. Fabrication of a Urethane-Based Heterogeneous Phantom Prototype

Here we describe the recipe we used to fabricate a phantom prototype mainly based on urethane rubbers. Indeed, it was developed in particular to check the possible suitability of this material, which could be preferred thanks to the SOS of the US wave propagation that is close to values usually considered for fabrication of US phantoms. The basic idea is to check whether a measurement on the phantom not immersed in water, being possibly less sensitive to artefacts on the return echo signal, can be performed even with quite strong attenuation.
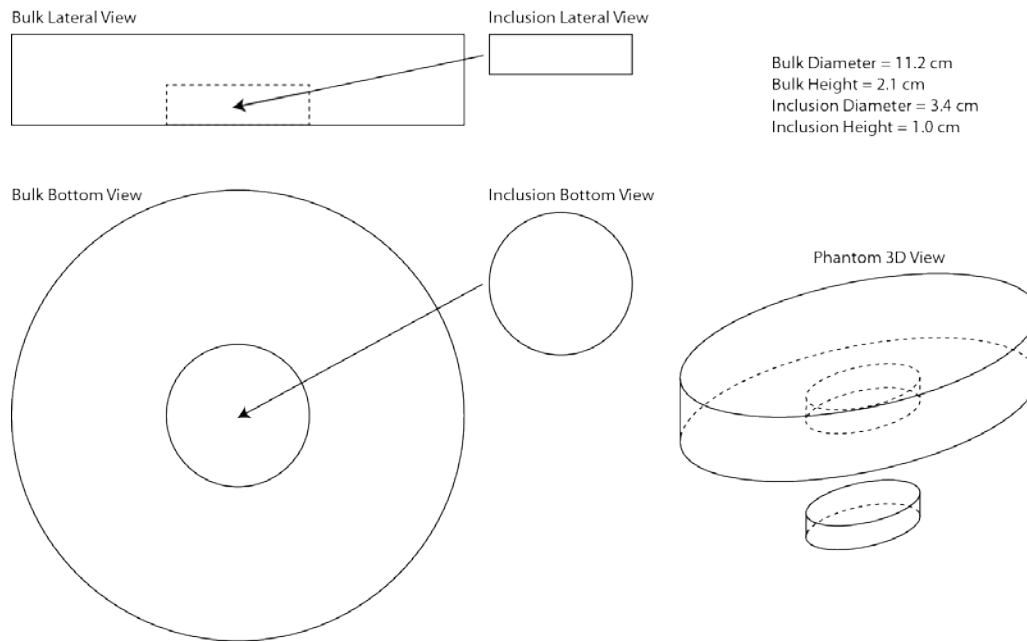
Figure 2 Layout of the phantom designed, in different views.

To fabricate the phantom, we stir part B for about 4 minutes in its tank before pouring. The required amount is determined by weight on a scale. TiO_2 powder is then added and mixed using an emulsionizer working at high speed. Then we add part A (measured by weight) and mix by hand for about 5 minutes. Finally, we degas the mixture in vacuum and afterward we pour the liquid in a new clean container of Nalgene plastic, which makes easier to remove cylinders from the jar thanks to reduced adhesion. The sample is cured at room temperature for 24 hours and then treated in the hoven at 65°C for 6 hours to eliminate surface stickiness.

In particular, the sample developed (see Figure 2) had a cylindrical shape with a base diameter of 112 mm (selected to remove possible echo artefacts coming from the boundary) and a height of 21 mm for a total volume of about 210 cm^3. To provide a scattering value of 10 cm^{-1}, 300 mg of TiO_2 powder was added to the volume. Absorption was obtained starting form UVO black pigment for urethane rubber (Smooth On). Firstly,10 μl of the pigment were diluted in 2 cm^3 of part B. Then 500 μl of this base mixture were added to the 108.25 cm^3 of part B. With the addition of 101.75 cm^3 of part A, the total volume had an absorption value of 0.42 cm^{-1} at 690 nm. To provide a cavity for the inclusion, a silicon Sylgard S184 cylinder of 34 mm diameter and 10 mm height was attached to the bottom of the Nalgene container and the urethane rubber was poured on top of it. After curing, the silicone cylinder was removed leaving a clean cavity. Using the same moulding container used for the silicone cylinder, the inclusion was prepared with Clear Flex 50 urethane rubber (Smooth-On, Part A and B 1:2 ratio). Being the total volume of the inclusion 9 cm^3, an amount of 38 mg of TiO_2 was added to give a reduced scattering coefficient of 15 cm^{-1}, while, following the same recipe as above, 20 μl of the base were added giving an absorption coefficient of 0.37 cm^{-1}. Considering the different hardness between Clear Flex 30 and Clear Flex 50 urethane rubbers, they may show US contrast when combined together due to a possible acoustic impedance mismatch.

At the end of the process, we have therefore a bulk phantom made of Clear Flex 30 and two possible inclusions to be inserted in the cavity, one made of Clear Flex 50 and one made of Sylgard S184 silicone rubber. In this way, it is possible to evaluate the US contrast with both combinations. Sylgard S184 (10:1 mixing ratio) has been selected among other silicone rubbers previously tested because of its lower attenuation to US propagation. Even if the lower echogenicity of P4 can be ascribed to a lower concentration of TiO_2 scattering centres, its preparation resulted complex, due to solidification processes occurring while mixing the two parts. To our purposes therefore Sylgard S184 appears more reliable.

5. Characterization of the Urethane-Based Phantom Prototype

OPTICAL CHARACTERIZATION

In this section, we report the optical characterization of homogeneous phantoms made of Clear Flex 30, Clear Flex 50 and Sylgard S184. We then inserted each inclusion in the bulk, measuring the phantom both with and without a thin layer of US gel in the cavity hosting the inclusion. As the gel in the cavity is necessary for US imaging to avoid the presence of air, this measurement allows us to evaluate possible artefacts in DOT due to the presence of such gel.

SETUP

The optical characterization was performed using a spectroscopic setup. It is composed of a supercontinuum laser coupled to a prism to provide light pulses at any selected wavelength in the range from 500 to 1100 nm. Light is then sent through a collimator into an optical fibre. It passes through a U-bracket where a variable optical attenuator is inserted in the free space and it is finally delivered to the sample through another optical fibre. To collect re-emitted photons we use a 1 mm diameter fibre, which is then coupled to a single-photon detector. The attenuator is set to have a maximum count-rate of about 700 kcps at all wavelengths selected, thus not exceeding the single photons statistics. More details about the setup can be found in [9].

All measurements were performed in the so-called "transmittance geometry" (i.e. photons are collected from the opposite plane with respect to the point where they are injected) in the 500-1100 nm range in steps of 5 nm. For each wavelength, 10 acquisitions of 1 s each were recorded.

The measurement of the US gel absorption spectrum (Cogel CUS 0250MF036, Comedical s.r.l.) was done using a spectrophotometer (Jasco V-750) in the same range.

DATA ANALYSIS

To retrieve the phantom optical properties, we summed up all repetitions to increase the signal-to-noise ratio and we fitted the resulting time-resolved curve to an analytical solution of the diffusion approximation of the transport equation for a homogeneous diffusive slab [10]. It is worth noting that we used the same procedure also for the heterogeneous phantom since the scope here was to check whether we recover a spectrum which is compatible with those of the bulk and of the inclusion, without artefacts coming from the presence of the US gel between bulk and inclusion.
To account for the laser pulse shape, detector response, broadening due to fibers and other effects, we previously convolve the instrument response function (acquired as in [11]) to the analytical model. The fitting algorithm is based on the minimization of the reduced χ^2 using a Levenberg-Marquardt routine [12]. The temporal range used is from 10% of the peak on the rising edge down to 1% of the peak on the falling edge of the acquired waveform.

To recover the US gel absorption spectra, we convert the absorbance value into the absorption coefficient following the Lambert-Beer law.

RESULTS AND DISCUSSION

Figure 3 reports the absorption (a) and reduced scattering (b) spectra of the samples: Clear Flex 30, Clear Flex 50 and Sylgard S184. The absorption spectra of both urethane rubbers show a nearly flat behaviour till 900 nm, where a broad absorption peak can be observed. A second peak at around 1020 nm can be also noticed. The absorption values at 690 nm are 0.42 cm^{-1} and 0.34 cm^{-1} for Clear Flex 30 and 50, respectively, as expected due to the addition of UVO pigment. The reduced scattering spectra are in line with expectations, following an almost monotonically decreasing power law (in agreement with empirical derivations of the Mie theory). As expected, μ_s' = 7.9 and 13.1 cm^{-1} at 690 nm for Clear Flex 30 and 50, respectively. For all phantoms, and in particular for the Clear Flex 50, in the 500-650 nm region, it is possible to notice a scattering-to-absorption coupling probably due to the larger instrument response function of the system in that range.
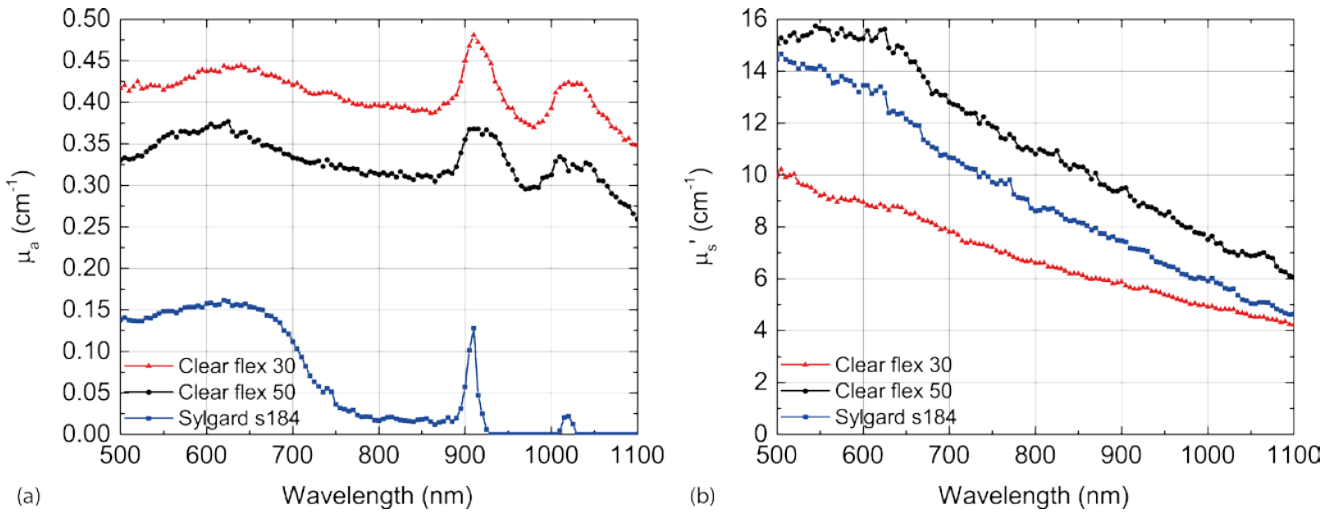
Figure 3 Absorption (a) and reduced scattering (b) spectra of Clear Flex 30, Clear Flex 50, and Sylgard S184.
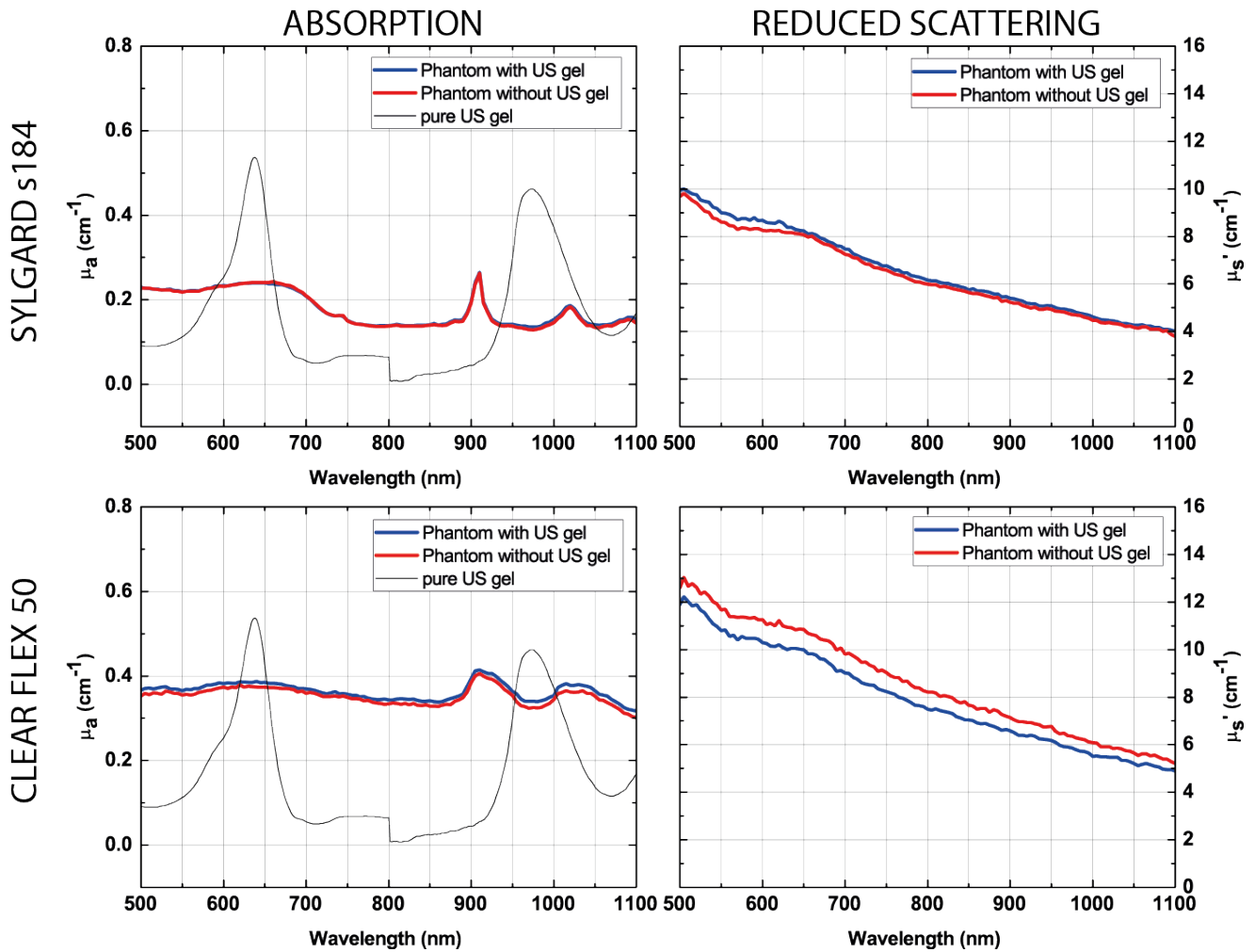

Figure 4 Absorption (left) and reduced scattering (right) spectra of the heterogeneous phantom with a Sylgard S184 (top row) or Clear Flex 50 (bottom row) inclusion. Measurements are carried out both with (blue curves) and without (red curve) a thin layer of US gel in the cavity hosting the inclusion.

For the Sylgard S184 phantom, there is a high-absorbing region (from 500 to 700 nm) due to the black silicone, while μ_a = 0.12 cm^{-1} at 690 nm. On the other hand, in the 750-1100 nm range, there is a very low absorption (here almost zero due to boundaries effects on such small samples) except from the 910 nm peak, a typical fingerprint of the silicone rubber. For what concerns the reduced scattering, the silicone phantom shows a linear decreasing trend with μ_s' = 10.76 cm^{-1} at 690 nm.

Figure 4 shows the absorption (left graphs) and reduced scattering (right graphs) spectra of the heterogeneous phantoms, where a Sylgard S184 (top graphs) or a Clear Flex 50 (bottom graphs) inclusion has been inserted alternatively. Looking at the absorption of the heterogeneous phantom with Sylgard S184 inclusion, we can notice the spectral features of the silicone rubber. However, the whole absorption spectrum is higher than that of the Sylgard S184 inclusion alone due to the combination with the Clear Flex 30 bulk, which has been designed to be more absorbing. Additionally, the effect of the US gel in between is totally negligible both in absorption and in reduced scattering spectrum since red and blue curve are overlapped, without any significant difference also where the US gel has strong absorption.

For the measurement done on the heterogeneous phantom with the Clear Flex 50 inclusion, we recover an absorption spectrum with an amplitude lower than the Clear Flex 30 (see Figure 3) since the inclusion has been designed to be less absorbing than the bulk, and with the same spectral features of urethane rubbers. Even in this case the effect of the US gel is almost negligible, since the difference between blue and red curves is flat, without the spectral features of the gel. This almost confirms that the difference is probably due to a different pressure on the sample in the two cases. Such a difference can indeed lead to a slight discrepancy of the sample's thickness, which can give a difference in the recovered reduced scattering and, to a lesser extent, also in the measured absorption coefficient.

CONCLUSION

The optical characterization of phantoms shows values of absorption and reduced scattering coefficients in line with those targeted by the recipe. The spectral features of both silicone and urethane rubbers are compatible with the needs of DOT. In addition, we can conclude that a thin layer of US gel can be inserted between the bulk and the inclusion to allow US investigations without particular impact on DOT.

ULTRASOUND CHARACTERIZATION

MATERIAL

Similarly to previous US measurements, a laboratory SSI Aixplorer V11 (S/N: SIA4115) was used with an SSI SL15-4 Gen 2 linear ultrasound probe (256 elements probe, element pitch 0.2 mm, central frequency 8.0 MHz, relative -6 dB bandwidth 80%). In some cases, an SSI SL10-2 Gen 1 low frequency linear transducer (192 elements probe, element pitch 0.2 mm, central frequency 6.0 MHz, relative -6 dB bandwidth 80%) was used to image the phantom with frequencies at which a lower US attenuation is expected. US gel has always been used when combining samples to improve the transmission of the US wave.

RESULTS AND DISCUSSION

Figure 5 (bottom) shows an image taken with the geometry shown in Figure 5 (top). The Aixplorer system was set to an SOS of 1250 m/s (i.e. to a value between silicone rubber and urethane rubber SOS). As expected, it is possible to notice a white horizontal line at a depth of less than 1 cm due to the impedance mismatch between Clear Flex 30 and Sylgard S184. However, the depth of the inclusion is underestimated due to the higher SOS in the Clear Flex 30 with respect to the Aixplorer setting. On the other hand, since the second horizontal white line is given by the impedance mismatch at the bottom of the inclusion, the inclusion thickness is overestimated due to the lower SOS. As desired, no impedance mismatch is recorded laterally, where the two Clear Flex 30 layers are in contact. However, this could also be due to the strong attenuation on the US signal experienced in this measurements, that could prevent the propagation of the US wave down to 21 mm. Indeed, the Sylgard S184 appears as an anechoic material (dark in the B-mode image), which is not in agreement with previous measurements reported in Sect. 3, thus confirming that probably the probe is not able to image deep through Clear Flex 30.
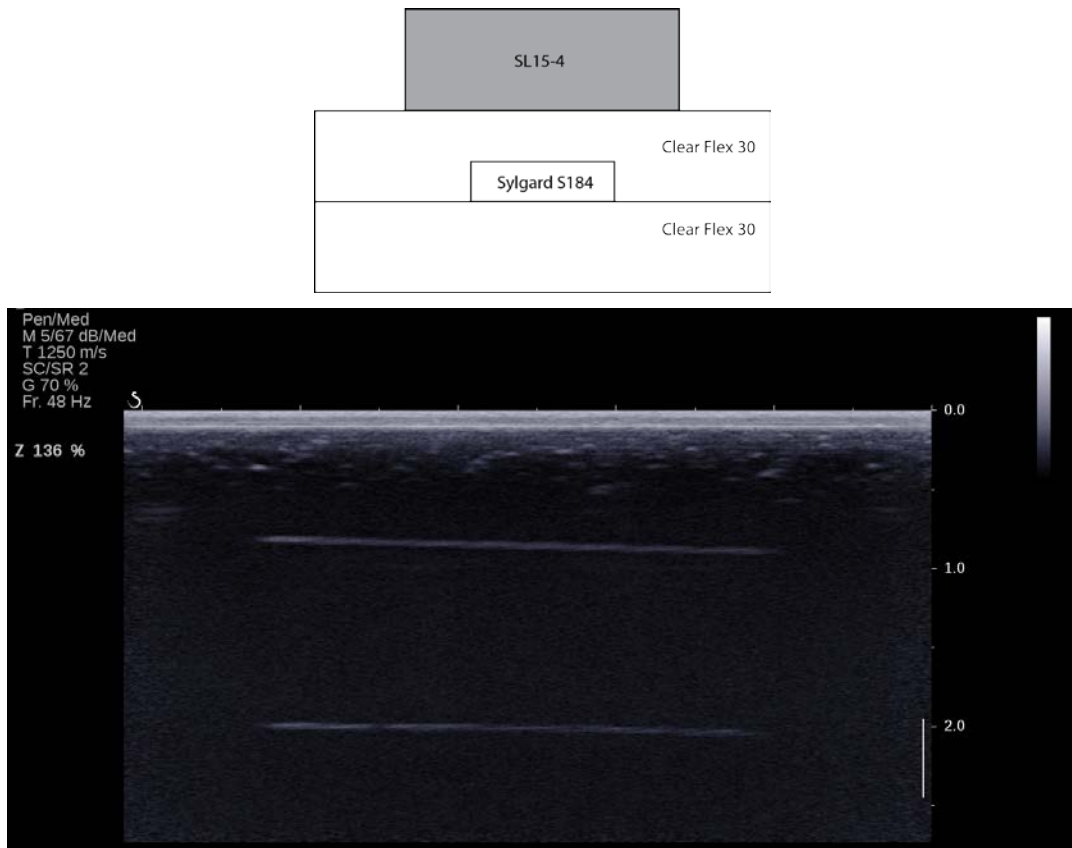
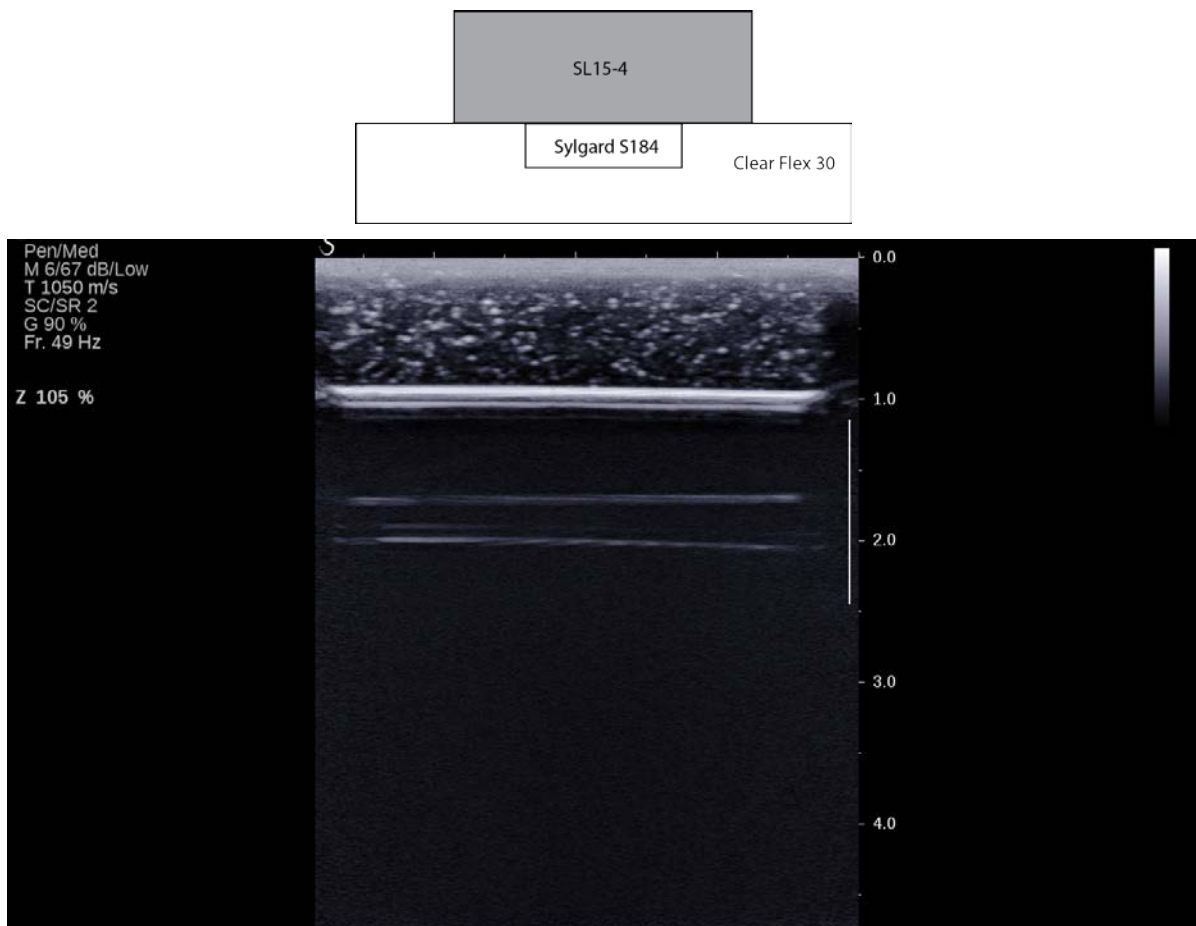*Figure 5 Measurement geometry (top) and corresponding US image (bottom).*

Figure 6 Measurement geometry (top) and corresponding US image (bottom).
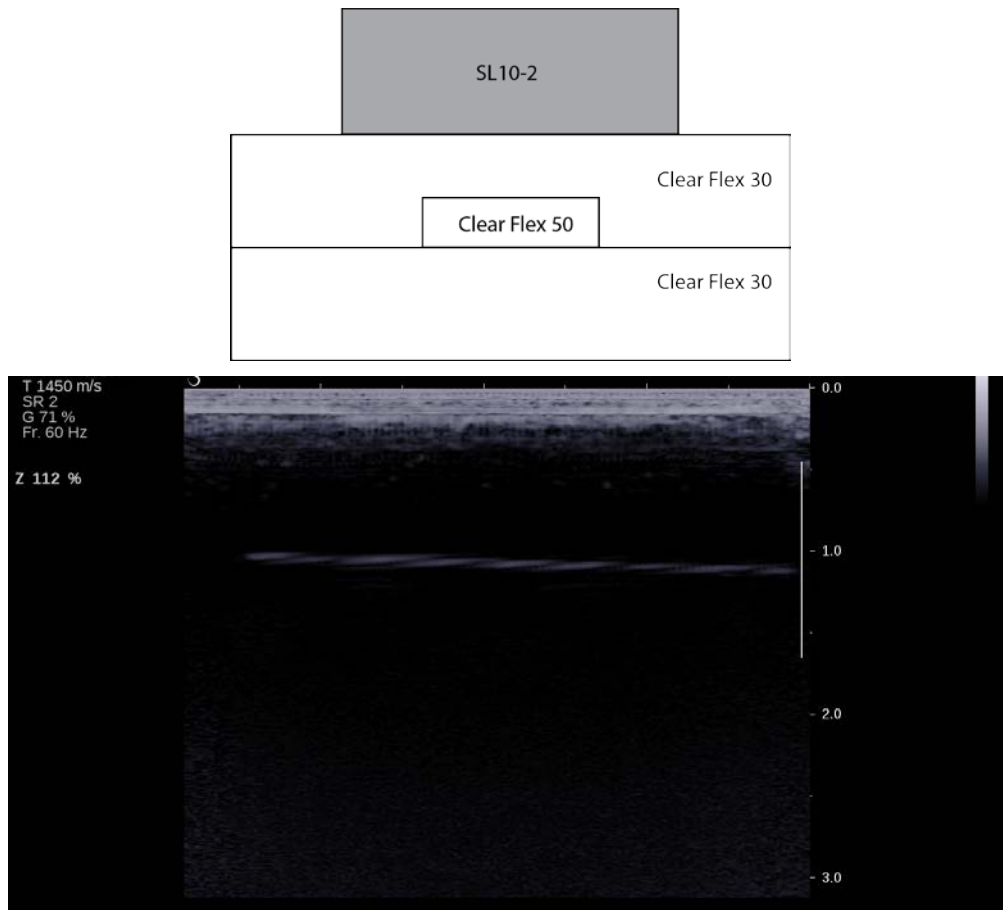
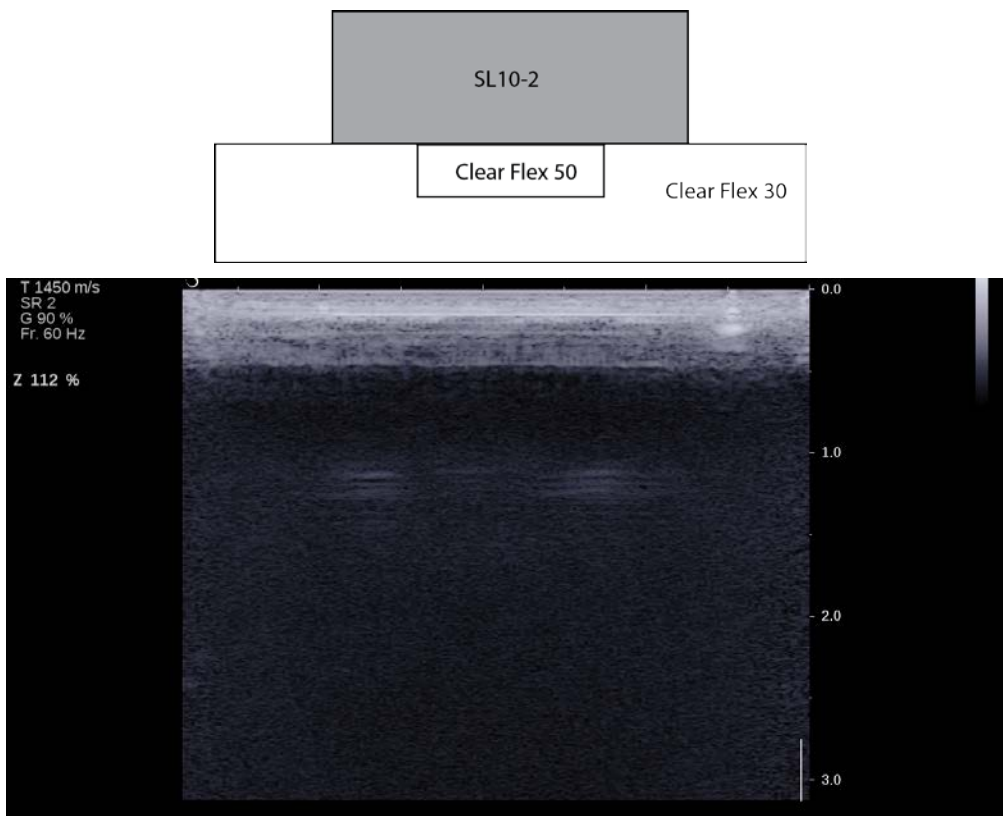*Figure 7 Measurement geometry (top) and corresponding US image (bottom).*

Figure 8 Measurement geometry (top) and corresponding US image (bottom).

Figure 6 (bottom) shows an image taken with the geometry shown in Figure 6 (top). Essentially the phantom was reversed, thus imaging the inclusion on top of the bulk. Here the Aixplorer is set to a SOS of 1050 m/s, almost matching the Sylgard S184 SOS. From the US image it is possible to see that the silicone rubber is imaged correctly in terms of thickness, thus proving that it is possible to obtain images with such a low SOS. Additionally, it is possible to notice the good echogenicity of the Sylgard S184, as resulted also in the measurements of Section 3. It is therefore possible to say that the measurement reported in Figure 5 is strongly affected by the attenuation introduced by the urethane rubber.

Figure 7 (bottom) shows an image taken with the geometry shown in Figure 7 (top). Now the inclusion is the one in Clear Flex 50. The SL 15-4 probe was also replaced with the SL10-2, at lower frequency, in order to be able to take an image. Indeed, as the attenuation of materials usually increases with the US frequency, with the SL 15-4 probe it was not possible to obtain an image. From this picture it is possible to see that the top face of the inclusion gives a return echo, as expected, but it is not possible to image the bottom surface, probably due to the even higher attenuation of the Clear Flex 50. Indeed, when reversing the phantom as in Figure 8, with the inclusion closer to the probe, the return echo of the interface between Clear Flex 50 and 30 is even lower, thus confirming the stronger attenuation in the Clear Flex 50.

CONCLUSION

The US characterization of phantoms shows that the water-clear urethane rubbers considered are not suitable to fabricate phantoms for use with the combined US-DOT system. In particular, notwithstanding the optimal value of the SOS, they present an excessive attenuation to the propagation of the US wave, preventing the penetration at the targeted depths for the inclusion. On the contrary, silicone rubbers can be considered as a suitable material notwithstanding the low SOS of about 1000 m/s. Indeed, the US characterization showed a good echogenicity level and penetration capability. Additionally, we proved that the Aixplorer system is able to image properly when the SOS is set at this level, thus ensuring the possibility to extract proper US images from phantoms in case we will opt for the use of this material.

6. Silicone-Based Phantom Prototype Fabrication and Characterization

INTRODUCTION

In the previous section, Sylgard S184 silicone rubber has been demonstrated as a suitable material to both optical and ultrasound phantoms. Here we describe the fabrication and characterization of a second heterogeneous phantom, which is this time completely based on Sylgard S184. As this material was already well assessed for diffuse optics applications, here we only investigate its US performance.

PHANTOM FABRICATION

The bulk phantom was made by pouring the material in a chamber (size 10 x 10 x 2 cm). Four cylinders (2 cm diameter, 0.1, 0.2, 0.4 and 0.6 cm height, respectively) were located on one 10 x 10 cm side. Thus, once the silicone was cured, 4 cylindrical holes were present on one side of the phantom. The volume of this phantom was made with the proper addition of base and hardener (10:1). The scattering properties (μ_s' = 10 cm^{-1}) were obtained adding 200 mg of TiO$_2$, while the absorption (μ_a = 0.1 cm^{-1}) was set mixing 1.1 g of Silicon Carbon Black previously diluted in a base (4.4 g in 100 g base). The cylindrical inclusions were obtained from aluminum molds. The four silicone cylinders had optical properties of μ_s' = 10 cm^{-1} and μ_a = 0.2 cm^{-1}. An additional layer of silicone (10 x 10 x 0.5 cm) was also made to be positioned on the inclusion side of the phantom to simulate fully embedded inclusions (see Figure 9). All the silicone preparations, before curing, were degassed in a vacuum chamber.
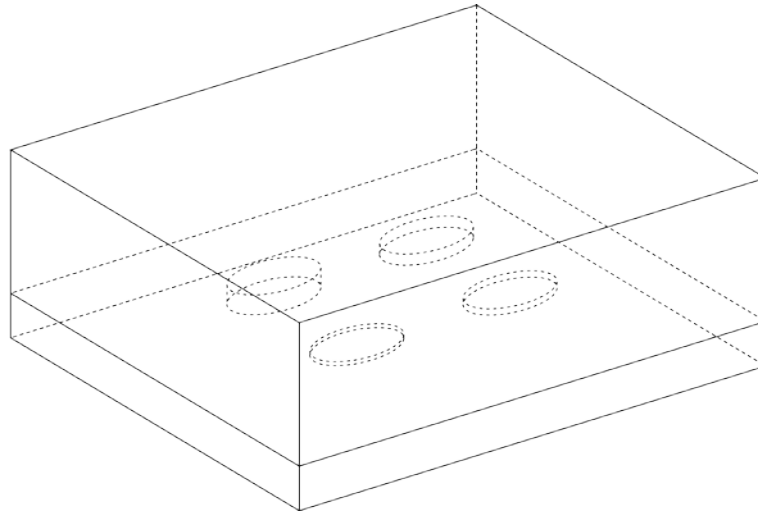
Figure 9 Layout of the Sylgard S184 silicone rubber phantom containing multiple cylindrical inclusions with different heights.
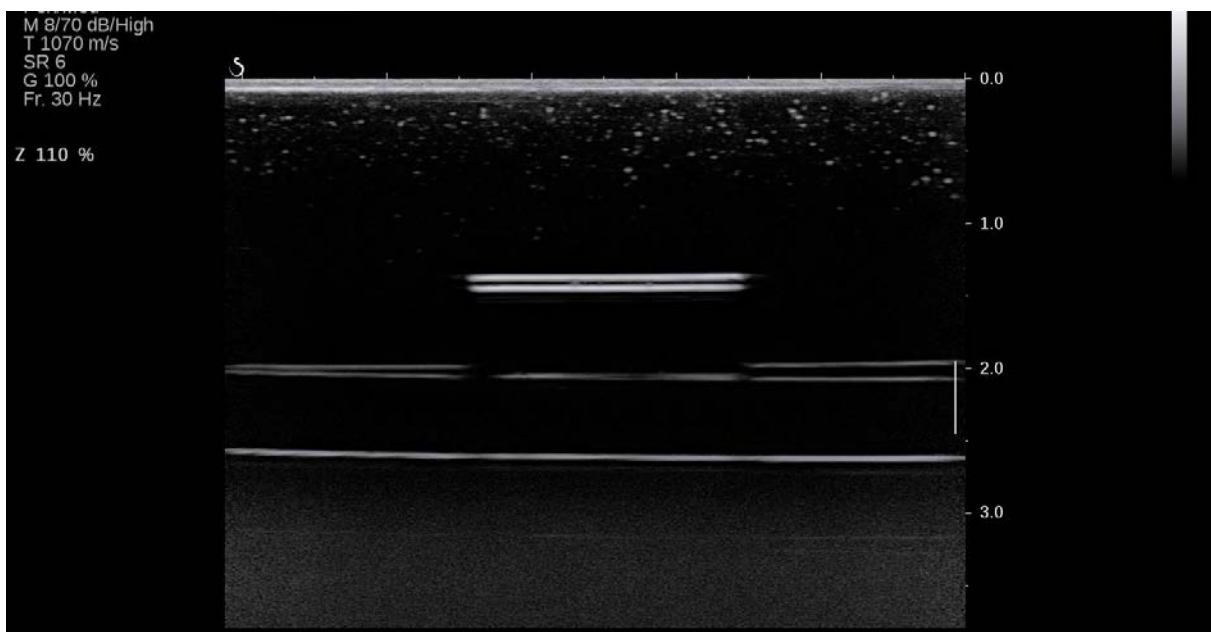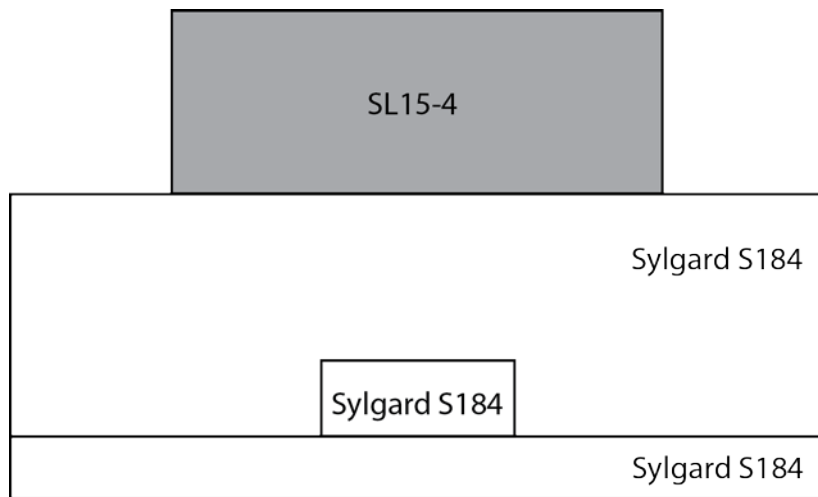

Figure 10 Measurement geometry (top) and corresponding US image (bottom).

RESULTS

US acquisitions were performed using a system similar to the one described in Section 5. US gel has always been used when combining samples to improve the transmission of the US wave. Figure 10 (bottom) shows an image taken with the geometry shown in Figure 10 (top) on a 0.6 cm height inclusion. Here the Aixplorer is set to an SOS of 1050 m/s, almost matching the Sylgard S184 SOS. From the US image it is possible to see that the inclusion thickness is imaged correctly. This time also other thicknesses are imaged correctly since the phantom is entirely made of the same material. This further confirms that it is possible to obtain images with such a low SOS.

However, in disagreement with measurements carried out in Sect. 3, the speckle distribution is not distinguishable within the lesion, as it was instead expected after measuring the relative echogenicity. This may be due to low penetration depth at the highest US frequencies, also confirmed by the fact that speckles can be imaged in the bulk in the first centimeter of depth (see Figure 10). However, surface echoes are strong enough to measure the dimension of the different phantom layers. It is possible somewhere to see a double white line at some interfaces between phantom layers. This may be due either to a not perfect adhesion between layers or also to the strong echo generating at the interface between silicone and the US gel, which may produce multiple transit echos. However, in this case the presence of the double white line is most probably due to a not perfect adhesion since on the left side slices seem almost in contact and the inclusion bottom is correctly imaged, probably due to its better adhesion with the bottom layer.

Images taken with other inclusions (data not shown) are comparable with that reported in Figure 10.

7. Conclusions

Different materials have been considered and tested with the goal to find out the best candidates for the fabrication of joint US-DOT phantoms. This has been done with particular attention to solutions allowing the fabrication of durable phantoms that can be useful in particular for the daily routine assessment during the clinical validation of the SOLUS system. To this purpose, only silicone rubbers (e.g. the Sylgard S184) offer proper performance to US propagation (proper echogenicity and attenuation). We also proved that it is possible to image properly inside phantoms even with a low SOS of about 1000 m/s using the SSI Aixplorer system, that is the reference system for SOLUS.

For the development of a kit of phantoms (D4.4, due at M18) there are therefore some different possibilities that can be evaluated during the next project year.

A first possibility is to use silicone rubbers to be able to fabricate durable and easy-to-use phantoms. This is feasible provided that different silicone rubber layers can be combined to obtain a proper impedance mismatch to be able to image the inclusion boundaries. Alternatively, the addition of some US scattering particles inside the silicone rubber could allow the fabrication of inclusions with different echogenicity with respect to the bulk phantoms, thus allowing inclusion imaging even without any impedance mismatch at the boundaries, provided that the US wave shows a sufficient penetration depth in the phantom to image its echogenicity. In the literature, different US scattering elements have been proposed, like: glass beads [13], nylon particles [14], silica particles [15], flour [16], etc. This addition is expected to alter the reduced scattering coefficient accordingly to the concentration, but it is also possible to properly calibrate the amount of titanium dioxide to obtain the desired optical scattering level.

Another possibility is to use materials already validated for both US and diffuse optics like agar [16]. Alternatively, since hydrogel phantoms have been proposed and validated for simulating both optical and ultrasonic properties of human tissues [7], they can be used for the implementation of the DOT-US systems characterization protocol. However, in both these cases, phantoms will be less durable and less suitable for measurements repeated over time or for sharing between laboratories.

7. References

[1] *A. Pifferi et al., "Mechanically switchable solid inhomogeneous phantom for performance tests in diffuse imaging and spectroscopy," J. Biomed. Opt. 20(12), 121304, 2015.*

[2] *A. Pifferi et al., "Performance assessment of photon migration instruments: the MEDPHOT protocol," Appl. Opt. 44(11), 2104-2114, 2005.*

[3] *J. Dong et al., "Diffuse correlation spectroscopy with a fast Fourier transform-based software autocorrelator," J. Biomed. Opt. 17(9), 097004, 2012.*

[4] *S. Konugolu Venkata Sekar et al. "Frequency offset Raman spectroscopy (FORS) for depth probing of diffusive media," Biomed. Opt. Express 25(5), 4585-4597, 2017.*

[5] *I. E. Iping Petterson, "Tissue phantoms to compare spatial and temporal offset modes of deep Raman spectroscopy," Analyst 140(7), 2504-2512, 2015.*

[6] *A. R. Selfridge, "Approximate material properties in isotropic materials," IEEE Trans. Sonics and Ultrasonics 32(3), 381-394, 1985.*

[7] *J. Boutet er al. "Bimodal organ phantom and associated production method," United States Patent no. 8,906,268 B2, Dec. 9, 2014.*

[8] *http://www.atslaboratories-phantoms.com/page8/page5/index.htm*

[9] *S. Konugolu Venkata Sekar et al., "Time-resolved diffuse optical spectrometer for clinical use," IEEE J. Sel. Top. Quantum Electron. 22(3), 7100609, 2016.*

[10] *D. Contini et al., "Photon migration through a turbid slab described by a model based on diffusion approximation. I. Theory," Appl. Opt. 36(19), 4587–4599, 1997.*

[11] *H. Wabnitz et al., "Performance assessment of time-domain optical brain imagers, part 1: basic instrumental performance protocol," J. Biomed. Opt. 19(8), 86010, 2014.*

[12] *W. H. Press et al., Numerical recipes in C, Cambridge Univ. Press 1, 3, 1988.*

[13] *K. Nam et al., "Ultrasonic attenuation and backscatter coefficient estimates of rodent-tumor-mimicking structures: comparison of results among clinical scanners," Ultrason. Imaging, 33(4), 233–250, 2011.*

[14] *K.V. Ramnarine et al., "Validation of a new blood-mimicking fluid for use in doppler flow test objects," Ultrasound Med Biol., 24(3), 451-459, 1998.*

[15] J.R. Cook et al., "Tissue-mimicking phantoms for photoacoustic and ultrasonic imaging," *Biomed. Opt. Express*, 2(11), 3193-3206, 2011.

[16] *M. Earle et al., "Agar ultrasound phantoms for low-cost training without refrigeration," African Journal of Emergency Medicine, 6, 18-23, 2016.*